Ultrasonics Sonochemistry 24 (2015) 132–139

Contents lists available at ScienceDirect

Ultrasonics Sonochemistry

journal homepage: www.elsevier.com/locate/ultson

Continuous precipitation of calcium carbonate using sonochemical reactor

S.R. Shirsath [a,1], S.H. Sonawane [b,*], D.R. Saini [c], A.B. Pandit [d]

[a] Department of Chemical Engineering, Vishwakarma Institute of Technology, 666 Upper Indira Nagar, Pune 411037, India
[b] Department of Chemical Engineering, National Institute of Technology, Warangal, AP 506004, India
[c] National Chemical Laboratory, Pashan, Pune 411008, India
[d] Chemical Engineering Division, Institute of Chemical Technology, Matunga, Mumbai 400019, India

ARTICLE INFO

Article history:
Received 28 August 2014
Received in revised form 7 December 2014
Accepted 7 December 2014
Available online 13 December 2014

Keywords:
Ultrasound
Nucleation
Crystal growth
Calcite
Morphology
Particle size

ABSTRACT

The continuous production of calcium carbonate ($CaCO_3$) by precipitation method at room temperature was carried out in a stirred reactor under ultrasonic environment and was compared with the conventional stirring method. The effect of various operating parameters such as $Ca(OH)_2$ slurry concentration, CO_2 flow rate and $Ca(OH)_2$ slurry flow rate on the particle size of $CaCO_3$ was investigated. The calcium carbonate particles were characterized by Fourier transform infrared (FTIR), wide angle X-ray diffraction (WXRD) and particle size. The morphology was studied by using scanning electron microscopic (SEM) images. The particle size obtained in the presence of ultrasonic environment was found to be smaller as compared to conventional stirring method. The particle size is found to be reduced with an increase in the concentrations of $Ca(OH)_2$ and increased with increasing CO_2 flow rate for both the methods. The slurry flow rate had a major effect on the particle size and the particle size decreased with increased slurry flow rate. Only calcite phase of $CaCO_3$ was predominantly present as confirmed by the characterization techniques for both the preparation methods. In most of the cases rhombohedral calcite particles were observed.

1. Introduction

Calcium carbonate ($CaCO_3$) is a widely used inorganic material in various industries and it is an abundant mineral comprising approximately 4% of the earths crust occurring as limestone, chalk, and biominerals [1,2]. Because of the harmless properties and inexpensiveness, it has been used for a variety of purposes and finds applications in diverse areas such as in the manufacture of toothpastes, lubricants, paints, textiles, plastics, adhesives, waste water treatment, rubber, ink, paper, ceramic materials, food and horticulture [3–6]. Therefore, the precipitation of calcium carbonate has received much attention of the researchers. Different applications of calcium carbonate necessitate various granulometric, physical and chemical properties. These specific requirements are generally achieved by preparing the substance under carefully controlled conditions with specific morphology, structure, specific surface area, particle size and particle size distribution etc. [4,7–8]. So as to achieve these specific properties, the kinetics of precipitation of calcium carbonate has been thoroughly investigated [9]. For the manufacturing of precipitated $CaCO_3$, the carbonation of lime is industrially practiced method [10–11]. In recent years nano-$CaCO_3$ has found large commercial importance because of its utility in diversified areas [12]. Inorganic nano-particle synthesis is a growing area of research and the change in the properties of materials with nanometric scale makes them increasingly suitable for a variety of applications. Some of the properties of nanomaterials like large surface area, different crystal geometries and hydrophobicity make them more suitable for the applications such as surface coatings, photocatalytic degradation, and catalytic activity [13].

The crystallization phenomenon of $CaCO_3$ is a complicated process involving three different phases of $CaCO_3$, namely calcite, aragonite, and vaterite. The operating variables such as pH of the solution, solute concentration, temperature of the reaction medium, and ionic strength of the media affect the crystal growth [1]. Three polymorphs of $CaCO_3$ like calcite, aragonite and vaterite have crystal structures of rhombohedral, orthorhombic and hexagonal respectively in nature. Calcite is the thermodynamically stable structure. Aragonite is mainly found in the biosynthetic $CaCO_3$

* Corresponding author. Tel.: +91 870 246 2626; fax: +91 20 25902178.
E-mail addresses: shirishsonawane09@gmail.com (S.H. Sonawane), dsaini2010@gmail.com (D.R. Saini).
[1] Current address: Department of Chemical Engineering, Sinhgad College of Engineering Vadgaon (BK), Pune 411041, India.

http://dx.doi.org/10.1016/j.ultsonch.2014.12.003
1350-4177/

such as shells and core and is a less stable form. The most unstable polymorph is vaterite, which rarely occurs in natural fields, but plays an important role in the calcium carbonate formation during precipitation [2,5]. There are various methods available for the $CaCO_3$ synthesis, such as batch carbonization [14], micro-emulsion [11], spray-carbonation, in situ deposition technique and ultrasound-assisted synthesis [12,13]. In carbonation process, CO_2 gas is passed through a slurry of $Ca(OH)_2$. The conventional carbonation process usually produces the precipitated $CaCO_3$ with spindle shape with particle size bigger than 2 μm [8].

However, there are a very few reports of continuous production of $CaCO_3$ which includes synthesis in Couette–Taylor reactor [15], Continuous-flow crystallizer [16], mixed suspension mixed product removal crystallizer (MSMPR) [17,18], MSMPR reactor with microwave radiation as a source of energy [19], and segmented flow tubular reactor [20]. On an industrial scale, it is necessary to produce large quantities of precipitated calcium carbonate (PCC). The issue of the production in large quantity can be resolved by producing $CaCO_3$ in a continuous process. It is also important to note that the batch process has number of limitations such as non-homogeneous mixing of three different phases (gas, liquid, solid), diffusion of solute through highly concentrated slurry, secondary nucleation, variation in the particle size, shape and distribution etc, which needs to be optimized from the batch to batch. Therefore, it is preferable to use continuous process over the batch process; hence number of attempts are made to shift from batch process to continuous process for the production of PCC.

The size distribution of nanometer particles is determined by the rate of nucleation and the subsequent crystal growth rate. Accelerated nucleation and inhibited growth, therefore, are the key factors for the synthesis of nanometer particles in aqueous solutions [21]. If the supersaturation and nucleation rates are too high, agglomeration becomes an important growth mechanism, leading to the formation of irregular aggregates. On the other hand, the particle size distribution is dependent on the degree of supersaturation in a reaction system [22]. For an ideal process, before the establishment of a steady-state nucleation rate, mixing of reactive ions should attain homogeneity at the molecular level. Process intensifying devices such as stirrers, jets, tee-mixers, static mixers, and rotating packed beds can be helpful for the improvement in the micromixing and homogenous distribution of reactive ions [22]. Hence, developing new processes and the reactors is always a challenging task for reactive precipitation reactions. Ultrasound can be effectively used for improving micro-mixing of CO_2 gas bubbles during calcium carbonate synthesis, which is demonstrated by Sonawane et al. [13]. Ultrasound synthesis has advantages over other methods in terms of narrower particle size distribution, smaller particle size, controlled morphology and rapid nucleation rate [23]. It has been generally observed that sonication promotes nucleation and inhibits crystal growth. Ultrasound was found to decrease the induction time, which is defined as the time elapsed between the creation of supersaturation and the appearance of crystals [24]. Kumar et al. [25] have utilized ultrasound as an intensification device to induce air into the reaction mass by breaking the interface of liquid/air for the generation of radicals. Lyczko et al. [26] have studied the effect of ultrasound on primary nucleation of potassium sulfate by measuring the induction time and metastable zone width of unseeded solutions.

Aim of the present work was to synthesize $CaCO_3$ particles in continuous mode by using ultrasonic reactor and conventional stirred tank reactor (CSTR). The effect of various operating parameters such as calcium hydroxide slurry concentration, calcium hydroxide slurry flow rate and CO_2 flow rate on the particle size and morphology has also been studied.

2. Experimental

2.1. Experimental setup

The experimental set up used for the continuous synthesis of $CaCO_3$ is shown in Fig. 1. This consists of a reactor with a sonication probe (Dakshin make, 240 W, 22 kHz) along with a gas distributor, magnetic stirrer and CO_2 gas supply. Small bubbles of CO_2 around 1 mm diameter were produced through the gas distributor. The ultrasound probe with tip of 10 mm diameter was used for the generation of ultrasonic waves. The progress of the reaction was continuously monitored using conductivity and pH measurement after regular intervals. Experiments were carried out in a continuous mode with and without ultrasound and the results were compared. While performing the experiments in the absence of cavitation, ultrasound probe was removed and only stirring was used. The temperature of the reactor was maintained constant during the experiments using the constant temperature bath, in which the CSTR assembly was immersed.

2.2. Synthesis of calcium carbonate particles

Initially $Ca(OH)_2$ (LR grade, High Purity Laboratory Chemicals, Mumbai) was dissolved in water to get the desired concentration. The suspension was completely mixed using stirrer (500 rpm) at a

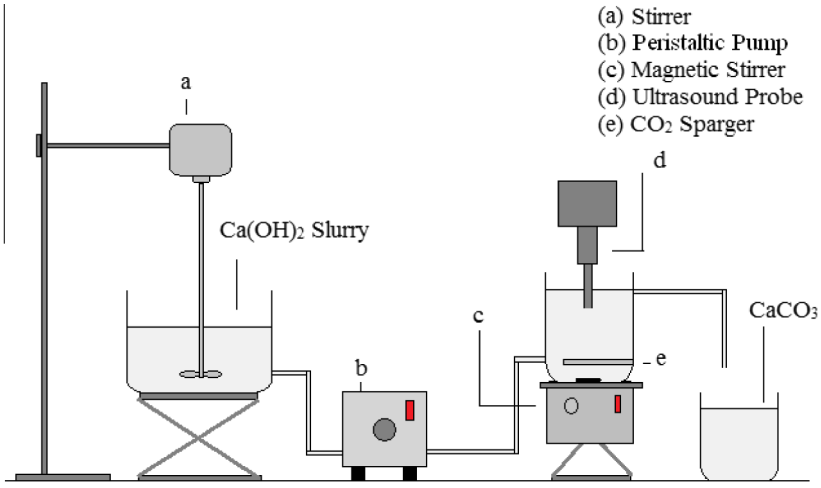

Fig. 1. Schematic of experimental setup for continuous production of $CaCO_3$ particles.

constant speed for 15 min so as to get a homogenous mixture. The carbon dioxide gas was introduced at the bottom of the reactor through a sparger. The $Ca(OH)_2$ slurry and CO_2 gas was fed to the reactor continuously and the product was continuously withdrawn from the reactor. At the starting of the experiment, the reactor was filled with calcium hydroxide slurry of desired concentration and then the flow of CO_2 into the reactor was started. The progress of the reaction was monitored by taking out the samples from the reactor at regular intervals of time as well as monitoring the pH and conductivity of the reaction mixture. The completion of the reaction was confirmed when the pH dropped to 7. Once the pH of the reaction mixture remained constant at 7, i.e. the steady state of the process, then the samples from the reactor were collected for the characterization purpose. The temperature of the reaction mixture in case of both the synthesis methods was maintained at 30 ± 2 °C. All the experiments were carried out in a continuous mode to study the effect of different operating parameters such as $Ca(OH)_2$ slurry concentration, $Ca(OH)_2$ slurry flow rate and CO_2 flow rate on the particle size and morphology of $CaCO_3$. The effect of $Ca(OH)_2$ slurry concentration was studied at fixed CO_2 flow rate of 45 Liter per hour (LPH) and $Ca(OH)_2$ slurry flow rate of 20 mL/min while the slurry concentration was varied from 1.96 to 5.66 wt%. The effect of CO_2 flow rate was studied for different flow rates of CO_2 (25–65 LPH) at fixed volumetric flow rate of 20 mL/min of $Ca(OH)_2$ slurry and the concentration of $Ca(OH)_2$ slurry was kept constant at 3.85 wt%. The actual volume of the reaction mixture was 700 mL indicating that the residence time of reactants in the reactor would be 35 min corresponding to 20 mL/min slurry flow rate. While in the study of the effect of $Ca(OH)_2$ slurry flow rate, which was varied from 12 to 28 mL/min, the residence time was 58–25 min respectively. Progress of the reaction was monitored by measuring the variations in pH and conductivity as a function of time. The obtained precipitate was washed two times with water and thrice with isopropanol in order to remove the impurities. After each washing, the $CaCO_3$ particles were separated by centrifugation. Finally $CaCO_3$ powder was dried at 80 °C for 24 h before it was used for characterization. The well known reaction mechanism for $CaCO_3$ synthesis consists of the following steps [10]:

$$Ca(OH)_2(s) \leftrightarrow Ca^{2+}(aq) + 2OH^-(aq) \quad (1)$$

$$CO_2(g) \leftrightarrow CO_2(aq) \quad (2)$$

$$CO_2(aq) + OH^-(aq) \rightarrow HCO_3^-(aq) \quad (3)$$

$$HCO_3^-(aq) + OH^-(aq) \rightarrow H_2O + CO_3^{2-}(aq) \quad (4)$$

$$Ca^{2+}(aq) + CO_3^{2-}(aq) \rightarrow CaCO_3(s) \quad (5)$$

2.3. Characterization

Samples from the reactor for characterization were collected only after the reactor has achieved a steady state condition (approximately after four to six residence times). Conductivity measurements were carried out by using a conductivity meter (SYSTRONICS conductivity meter 304). XRD diffraction patterns of $CaCO_3$ samples were recorded by means of powder X-ray diffractometer (Philips PW 1800) between 20° and 80° with a scan rate of 2°/min. The Cu Kα radiation (LFF tube 35 kV, 50 mA) was selected for the XRD analysis. FTIR analysis of samples were carried out (SHIMADZU 8400S) in the region of 4000–400 cm^{-1}. The morphology of $CaCO_3$ particles was investigated by using Scanning Electron Microscopy (SEM) (JEOL JSM, 680LA 15 kV, magnification 10,000×). The particle size distribution measurements were carried out by Malvern Zetasizer Instrument (Malvern Instruments, Malvern, UK).

3. Results and discussions

3.1. Analysis of pH and electrical conductivity in presence and absence of ultrasound

During the carbonation process the reduction of ions present in the process takes place, therefore the process can be monitored by the measurement of electrical conductivity of the aqueous suspension [27]. Also the hydroxyl ions released due to calcium hydroxide dissociation are consumed for the calcium carbonate production, allows the study of reactive process on the basis of the pH values [14]. Hence in order to study the progress of the reaction and the phenomena of nucleation and crystal growth, the conductivity and pH of the reaction mixture was monitored as a function of carbonation time. Figs. 2 and 3 show the variation of conductivity and pH during the carbonation reaction with respect to time for 3.85 wt% slurry concentration and 45 LPH of CO_2 flow rate for both methods of synthesis.

For both, conventional and ultrasound assisted synthesis methods, the value of conductivity drastically dropped with time (Fig. 2). This drop in conductivity indicates that the massive nuclei of calcium carbonate are just formed and getting attached to the

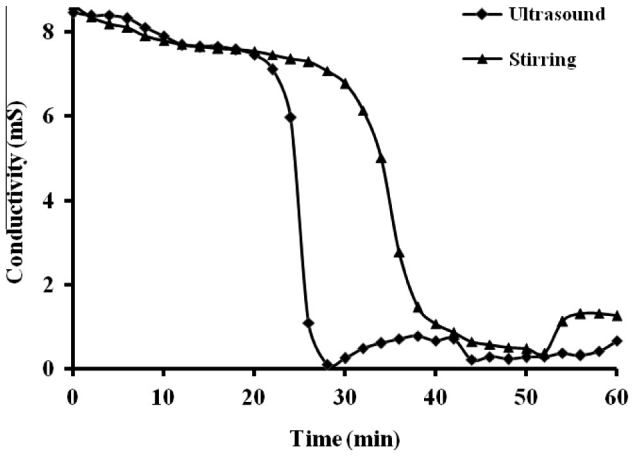

Fig. 2. Variation of electrical conductivity versus carbonation time.

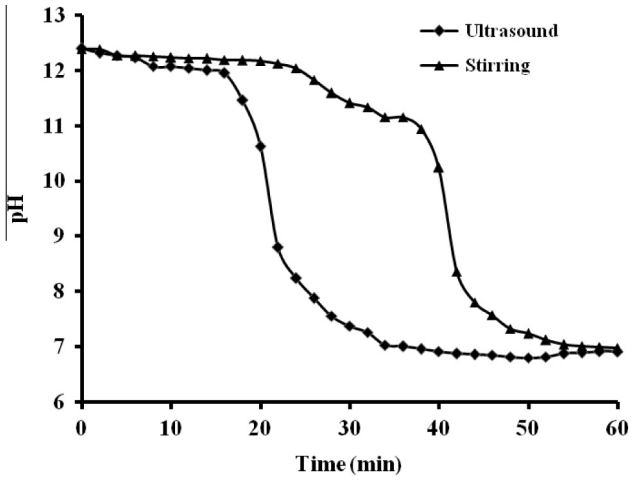

Fig. 3. Variation of pH versus carbonation time.

surface of particles of $Ca(OH)_2$ leading to the formation of a gel impeding the transfer of Ca^{2+} and OH^- ions [12–13,28]. Also, the conductivity reverted quickly, as a result of rapid de-agglomeration of the gel due to the further dissolution of $Ca(OH)_2$ particles ($Ksp_{Ca(OH)2} > Ksp_{CaCO3}$) and substantial increase in the number of nuclei of calcium carbonate with blowing CO_2 into the reactor. The size distribution of nanometer particles is determined by the rate of nucleation and the subsequent growth. The fast nucleation produces smaller particles wherein if the growth rate is predominant, the crystallite usually is composed of larger particles [21]. The value of conductivity reached to a minimum at the pH near 7, since the $Ca(OH)_2$ phase completely disappeared and the carbonation reaction was finished.

For stirring operation, delayed nucleation is observed with lower magnitude drop in conductivity as compared to ultrasound assisted carbonation process, indicating that the precipitation is slower in the absence of cavitation [29]. It is attributed to the formation of the larger number of the nuclei of calcium carbonate in the presence of ultrasonic irradiations compared to conventional stirring. During the ultrasound irradiation, bubbles are formed in the reaction mixture which grow to a certain size and then collapse violently. The collapse of bubbles produces intense local heating and high pressures, as well as very high cooling rates. The early nucleation because of early supersaturation attained in the presence of ultrasound is attributed to rapid local cooling rates, in the range of 10^7–10^{10} K/s, associated with the bubble collapse that drastically reduces the solubility of Ca^{2+} and thus the solution reaches its supersaturation. Localized pressure increase reduces the crystallization temperature and the cavitation events allow the excitation energy barriers associated with this nucleation to be surmounted [23]. The pronounced effect of ultrasound was evident from these results.

Further, pH value of the reaction mixture as a function of time for carbonation reaction with and without ultrasonication is reported in Fig. 3. From Fig. 3 it can be seen that the patterns of carbonation reaction with and without ultrasonication are similar for pH. The pH value remained constant at around 12–12.5 during most of the carbonation time. This is attributed to the lesser dissolution rate of $Ca(OH)_2$ than the rate of its addition to the reactor, hence the concentration of OH^- ions remains constant. This indicates that the pH is an independent parameter and not influenced by the transfer of ions and it is only dependent on OH^- ion concentration [12,13,28]. Both conductivity and pH decreased rapidly due to steady decrease of $Ca(OH)_2$ which resulted into the formation of Ca^{2+} and OH^- ions and further gradual decrease of Ca^{2+} and OH^- contents in the solution [8]. At the pH value of around 7, the $Ca(OH)_2$ phase completely disappeared and the carbonation reaction was completed resulting in the formation of $CaCO_3$. Similar trend of variation of conductivity and pH with time was observed for other experiments also.

3.2. XRD analysis of calcium carbonate particles

The wide angle X-ray diffraction pattern was used to investigate the phase structures of prepared $CaCO_3$ particles. Fig. 4 shows the X-ray diffraction patterns of $CaCO_3$ particles prepared by ultrasonic and conventional stirring method. Fig. 4A depicts the XRD patterns of $CaCO_3$ for 3.85 wt% $Ca(OH)_2$ slurry concentration (CO_2 flow rate = 45 LPH, $Ca(OH)_2$ slurry flow rate = 20 mL/min), Fig. 4B shows XRD patterns for 55 LPH CO_2 flow rate (3.85 wt% $Ca(OH)_2$ slurry concentration and $Ca(OH)_2$ slurry flow rate = 20 mL/min), and Fig. 4C is for 16 mL/min slurry flow rate (3.85 wt% $Ca(OH)_2$ slurry concentration and CO_2 flow rate = 45 LPH) for both methods of synthesis.

For both the preparation methods at different operating conditions of $Ca(OH)_2$ slurry concentration, CO_2 flow rate and $Ca(OH)_2$ slurry flow rate, the XRD pattern shows the peaks at $2\theta = 23.1°$, 29.4°, 34.2°, 36°, 39.5°, 43.2°, 47.6°, 48.6°, 57.6°, 60.9°, and 64.9°. All these peaks are attributable to calcite phase of calcium carbonate [30–32] indicating that the calcite phase was predominantly formed during carbonization process. These diffraction data are in good agreement with those of JCPDS PDF2 standard card (005-0586) (Mineral Powder Diffraction File Data Book ICDD No. 5-586) [31]. Further, in all cases it is also observed that the intensity of the peaks in XRD patterns in the case of ultrasound assisted method is significantly lower compared to that of conventional method. Additionally broadening of XRD peaks is observed in the case of ultrasound assisted method indicating the smaller particle size of $CaCO_3$ particles with less crystallinity [33].

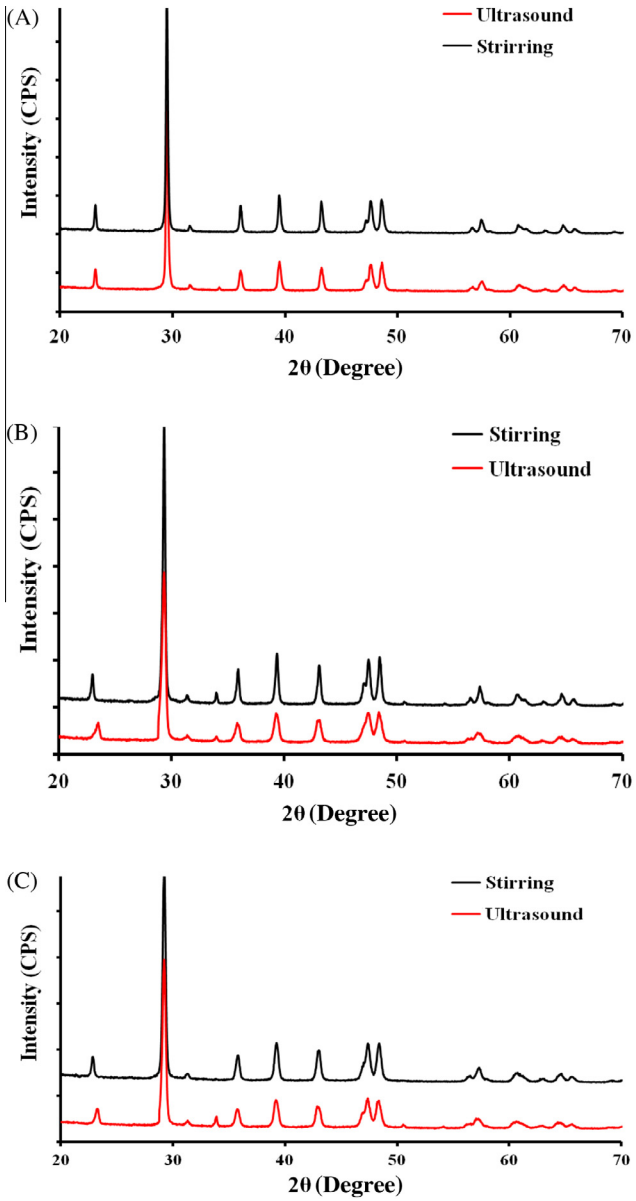

Fig. 4. X-ray diffraction patterns of $CaCO_3$ particles (A) 3.85 wt% $Ca(OH)_2$ slurry concentration, (B) 55 LPH CO_2 flow rate, and (C) 16 mL/min $Ca(OH)_2$ slurry flow rate.

3.3. FTIR analysis of calcium carbonate particles

The FTIR spectra of calcium carbonate particles prepared by ultrasonic and conventional stirring method and mixed sample of

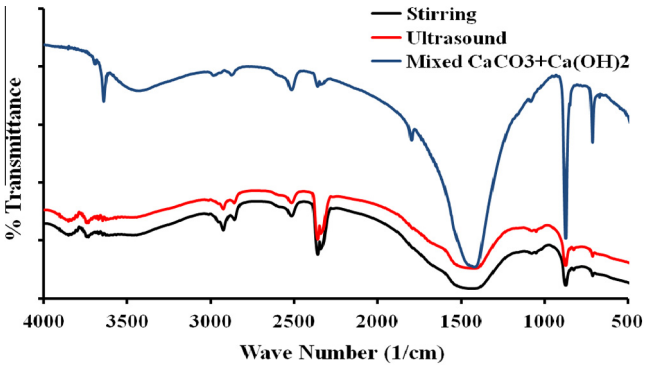

Fig. 5. FT-IR spectra of $CaCO_3$ particles.

90 wt% $CaCO_3$ and 10 wt% $Ca(OH)_2$ are depicted in Fig. 5. As reported in the literature [28,31,32,34–36] the absorption bands in the region of 712–717 and 874–876 cm^{-1} are assigned to characteristic ν4 and ν2 absorption of CO_3^{2-} ions respectively and 1430–1460 cm^{-1} are assigned to ν3 absorption bands of calcite. In the present work, results of FTIR analysis shows main absorption peaks located in the regions of 715–717, 876–877 and 1430–1496 cm^{-1}. Therefore absorption bands in the region of 715–717 cm^{-1} are attributed to characteristic ν4 absorption of CO_3^{2-} ions, while the bands in the region of 876–877 cm^{-1} may be assigned to the characteristic ν2 absorption of CO_3^{2-} ions. The absorption bands in the region of 1430–1496 cm^{-1} can be assigned to ν3 absorption bands of calcite. The presence of these absorption bands confirms the formation of calcite phase of $CaCO_3$ particles by ultrasound assisted and conventional stirring method. Moreover the typical absorption band at 1086 cm^{-1} for the ν1 band of amorphous $CaCO_3$ was not seen, indicating the absence of amorphous $CaCO_3$ in the samples. Combining the FTIR and XRD results above, it is evident that the $CaCO_3$ particles formed in the study are predominantly the calcite crystal form.

Additionally in order to estimate the unreacted $Ca(OH)_2$ at the end of carbonization reaction, the FTIR patterns of $CaCO_3$ prepared by ultrasound and conventional stirring methods were compared to the FTIR pattern of synthetic mixture of 90 wt% $CaCO_3$ and 10 wt% $Ca(OH)_2$ and is depicted in Fig. 5. The characteristic peak for $Ca(OH)_2$ reported by Gu et al. [36] is observed at 3654 cm^{-1}. In the present work, in case of the synthetic mixture of 90 wt% $CaCO_3$ and 10 wt% $Ca(OH)_2$, the sharp peak is observed at 3645 cm^{-1} attributing to the presence of $Ca(OH)_2$ in the sample. However, in the FTIR pattern of $CaCO_3$ produced by ultrasound assisted and conventional stirring method, this peak is completely diminished indicating the complete conversion of $Ca(OH)_2$ during the carbonization reaction.

3.4. Effect of ultrasound on particle size of $CaCO_3$ against conventional carbonation method

3.4.1. Effect of $Ca(OH)_2$ slurry concentration

The effect of $Ca(OH)_2$ slurry concentration (1.96–5.66 wt%) on the morphology and particle size of calcium carbonate was investigated at fixed volumetric flow rate of 20 mL/min. Further the CO_2 flow rate was maintained constant at 45 LPH and the experiments were performed with the use of ultrasound as well as conventional stirring. Fig. 6 depicts the SEM images of the $CaCO_3$ particles at different $Ca(OH)_2$ slurry concentrations with both the methods of synthesis. It has been observed that the cubical/rhombohedral $CaCO_3$ particles are formed with both methods of synthesis. It has been clearly observed from SEM images that the particle size, in case of ultrasound, is decreased with an increase in the $Ca(OH)_2$ slurry concentration from 2.92 to 4.76 wt%. Also in case of conventional method of synthesis, the particles size is found to be decreased with an increase in the $Ca(OH)_2$ slurry concentration from 2.92 to 3.85 wt% and again it is increased for 4.76 wt% $Ca(OH)_2$ slurry concentration. The probable reason is explained in the subsequent paragraph. There are mixed results reported in the literature related to the type of crystals formed in presence and absence of ultrasound. Some authors have obtained similar crystals in the presence and absence of cavitation whereas others have reported substantial differences [23]. Nishida [37] has reported the same morphology for calcium carbonate crystals under ultrasonic irradiation and mechanical stirring. However in a study conducted by Enomoto et al. [38] it was found that the ultrasound promoted the goethite formation while magnetic stirring favoured the formation of magnetite during the oxidation of iron hydroxide.

Table 1 shows the particle sizes for both the methods of synthesis for some of the representative samples. As seen in Table 1 the

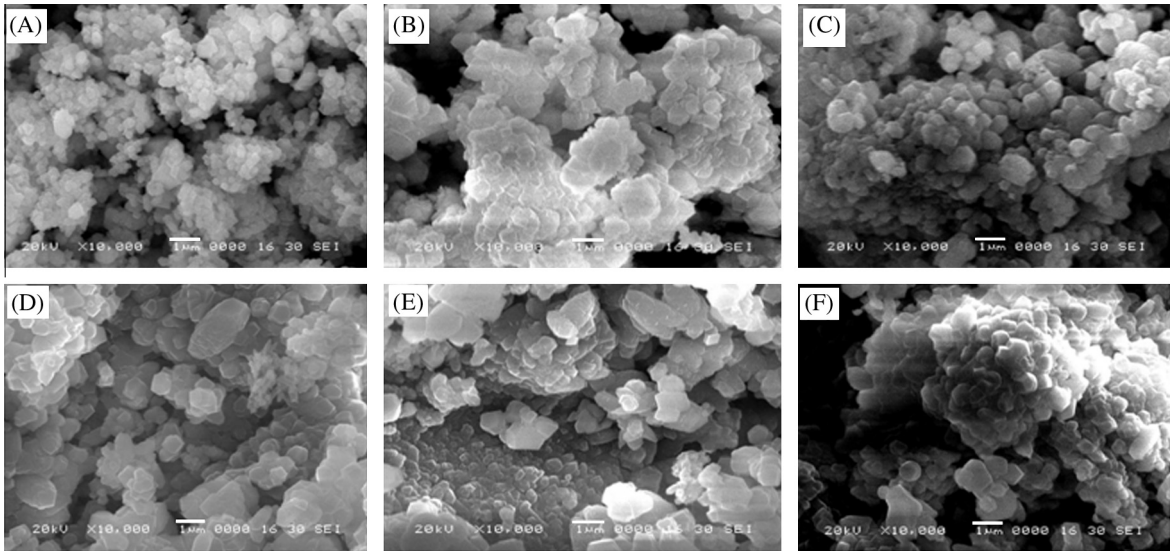

Fig. 6. SEM images of $CaCO_3$ particles for (A) 2.92 wt% (ultrasound), (B) 3.85 wt% (ultrasound), (C) 4.76 wt% (ultrasound), (D) 2.92 wt% (stirring), (E) 3.85 wt% (stirring), and (F) 4.76 wt% (stirring) $Ca(OH)_2$ slurry concentration.

Table 1
Particle size of $CaCO_3$ particles.

Parameter	Particle size (nm)	
	Stirring	Ultrasound
Slurry concentration (wt%)		
1.96	1314	1018
2.92	1157	744
3.85	601	371
4.76	967	366
5.66	1151	858
CO_2 flow rate (LPH)		
35	575	132
45	601	371
55	521	373
65	1144	918
Slurry flow rate (mL/min)		
12	971	685
16	691	423
20	601	371
24	577	244

particle size is found to be reduced with an increase in the $Ca(OH)_2$ slurry concentration to a certain level. In the case of mechanical stirring and for ultrasound assisted method, the particle size is found to be reduced till a slurry concentration of 3.85 and 4.76 wt%, by weight respectively. The probable reason for this may be that the excess of $Ca(OH)_2$ in the ultrasound assisted reaction results in the excess of Ca^{2+} ions in the solution. These excess Ca^{2+} ions may be adsorbed on the preferred faces of the calcium carbonate particle and then the adsorbed ions inhibit the face growth of a particle leading to a reduction in the mean particle size [7,15]. Also, the particle size of $CaCO_3$ particle in the presence of ultrasound is observed to be smaller than that of conventional method of synthesis. The particle size of $CaCO_3$ particles is generally determined by the rate of nucleation and the subsequent growth. The ratio between the rates of these two processes determines the size and number of the particles. Accelerated nucleation and inhibited growth, therefore, are the key factors for the synthesis of nanometer particles in aqueous solutions [21]. In the presence of ultrasound it is possible to attain early nucleation at faster rate leading to formation of large number of nuclei and it limits the particle growth which forms the nanometer size particles. Also the particle size is dependent on the distribution of supersaturation in a reaction system. For an ideal process, before the establishment of a steady-state nucleation rate, the mixing of reactive ions should attain homogeneity at the molecular level. The use of ultrasound can enhance the mixing and attains fairly uniform distribution of supersaturation in the reaction medium. This leads to the formation of nanometer sized $CaCO_3$ particles. However this is not the case in conventional synthesis of $CaCO_3$, therefore comparatively larger sized particles are obtained. Further ultrasound can enhance the supersaturation of Ca^{2+} and solute transfer rate at lower slurry concentration. The considerable reduction in the particle size of $CaCO_3$ particle is ascribed to the significantly improved micromixing, enhanced solute transfer rate, rapid nucleation, and the formation of large number of nuclei due to the physical effects of the ultrasound. The possible reason for this reduction in the particle size is also attributed to the fast kinetics of the ultrasound assisted reaction, which does not, provides enough time for the growth of $CaCO_3$ particle leading to an ultimate reduction in the particle size [35].

Moreover, when the concentration of the $Ca(OH)_2$ was increased to 4.76 wt% in the case of conventional stirring and to 5.66 wt% in case of ultrasound method, the increase in the particle size is observed. At higher concentration of $Ca(OH)_2$, large number of dissolved particles of $Ca(OH)_2$ may interfere with the effect of ultrasonication resulting in formation of a continuous gel-like network in the solution (due to coexistence of $Ca(OH)_2$ and $CaCO_3$ particles), which could not be well dispersed with the ultrasonication, leading to a nonuniform nucleation [12]. Similar reasons are also applicable in case of stirring as massive solid particles of $Ca(OH)_2$ and $CaCO_3$ coexist in the solution and agglomerate with each other, resulting in non homogeneous mixing.

The difference in the sizes determined by particle size analyzer and SEM images would be due to the coagulation or agglomeration of the particles during sample preparation for particle size measurements [2].

3.4.2. Effect of CO_2 flow rate

The effect of CO_2 flow rate on the particle size and morphology of calcium carbonate was studied for different flow rates of CO_2 (25–65 LPH) for both synthesis methods. The volumetric flow rate of $Ca(OH)_2$ slurry was maintained at 20 mL/min with 3.85 wt% slurry concentration. Fig. 7 shows the SEM images of the $CaCO_3$ particles at 55 LPH CO_2 flow rate with both methods of synthesis. From Fig. 7A it is seen that with ultrasound rhombic and distorted cubes of $CaCO_3$ particles are formed whereas with the conventional method (Fig. 7B) plate like particles are formed. The particle morphology changed from rhombohedral with ultrasound to stacked plates with the stirring method of synthesis. The change in morphology of $CaCO_3$ with the preparation method may be attributed to the dissolving rate of CO_2 at different conditions. The lower carbonation rate with conventional stirring method may provide a favorable condition for the formation of plate-like particles. As reported by Wen et al. [39] a lower value of $[Ca^{2+}]/[C]_T$ is favorable

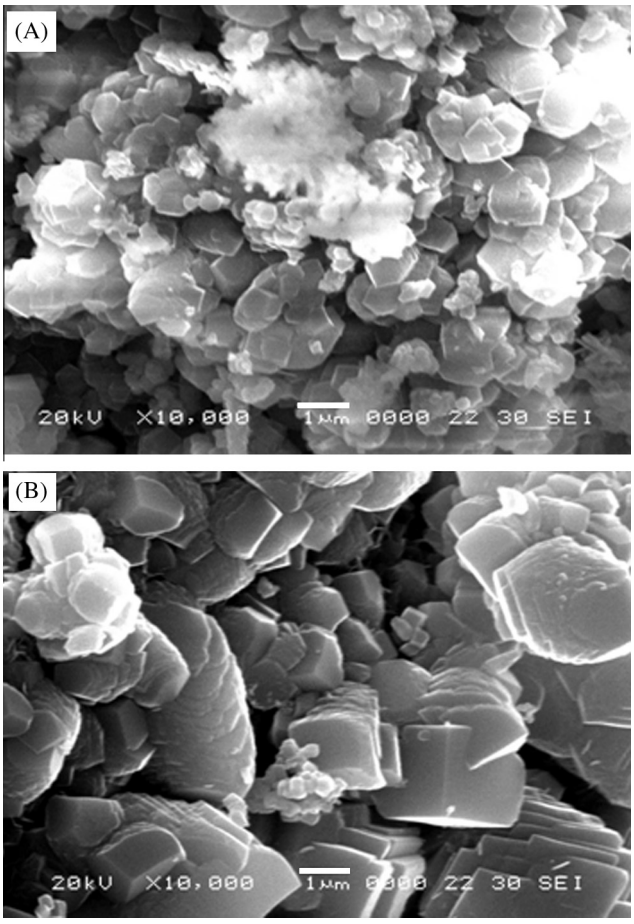

Fig. 7. SEM images of $CaCO_3$ particles for CO_2 flow rate of 55 LPH (A) ultrasound, and (B) stirring.

for the formation of plate-like $CaCO_3$ particles where Ca^{2+} is the concentration of calcium ions in the reactor and $[C]_T$ refers to the total concentration of carbon-containing components in solution. As discussed earlier ultrasound can enhance the supersaturation of Ca^{2+} which means that with ultrasound the ratio of $[Ca^{2+}]/[C]_T$ is higher as compared to conventional stirring method hence lower value of this ratio associated with stirring may be responsible for formation of plate-like particles.

Also, from SEM images, it is observed that the particle size of $CaCO_3$ is smaller in case of ultrasound method of synthesis. From Table 1 it can be clearly seen that the particle size is larger with conventional method than that of sonochemical method. It is believed that the precipitation process is controlled by the mass transfer at the gas liquid interface [10,40]. For conventional method, CO_2 concentration might be less in the reaction zone due to higher film resistance at gas–liquid interface compared to sonochemical method where reduction in the gas–liquid film thickness takes place. In this three phase reaction, the dissolution of $Ca(OH)_2$ is improved because of the rigorous mixing generated by ultrasound. This rigorous mixing improves the transport of gas molecules to the solid surface that leads to an increase in the mass transfer and therefore the overall reaction rate. Further the shock waves and microjets generated due to cavitational effect of ultrasound can accelerate the motion of the liquid molecules and increase molecular impacts so as to speed up the reaction. The thickness of the stagnant film and the adsorption layer adjacent to the growing crystal surface depends on the relative solid–liquid velocity and is decreased in the presence of ultrasound [41]. The particle size is found to be higher with an increasing CO_2 flow rate. This may be because the solubility of CO_2 is constant at any given conditions. At room temperature, the solubility of carbon dioxide is about 90 cm^3 of CO_2 per 100 mL of water. Hence, when the flow rate of CO_2 is increased some amount of the interacted CO_2 gas cannot be absorbed by water but it runs out of the solution directly [42]. Whereas at low flow rate the consumption rate of CO_2 gas by unit mass of $Ca(OH)_2$ for the reduction is very close to its absorption rate. The results are in good agreement with those reported by Triveni et al. [43] but different from those reported by He et al. [12] where particle size decreased with CO_2 flow rate. As reported by Feng et al. [40] the increase of CO_2 flow rate may not always result in smaller particle size.

Additionally with both the methods, there is large increment in the particle size at higher gas flow rate (65 LPH). For the formation of $CaCO_3$, the CO_2 molecules must enter the phase containing the Ca^{2+} ions and therefore mass transport resistance is a very important parameter. The resistance to CO_2 transfer into the water can be stated in terms of viscosity and the viscosity of CO_2 is less compared to the viscosity of water. At very high CO_2 flow rate, the penetration of CO_2 molecules in water phase is low due to higher mobility of CO_2 molecules with respect to water and the viscosity difference which ultimately results into CO_2 bypassing the solution [43]. This results in the nucleation at limited locations and this continues to grow leading to formation of larger sized $CaCO_3$.

3.4.3. Effect of $Ca(OH)_2$ slurry flow rate

The effect of $Ca(OH)_2$ slurry flow rate is studied for different flow rates 12–28 mL/min (3.85 wt% $Ca(OH)_2$ slurry concentration and CO_2 flow rate 45 LPH). SEM images of the $CaCO_3$ particles at $Ca(OH)_2$ slurry flow rate of 16 mL/min for both the methods of synthesis are shown in Fig. 8. SEM images shows two different morphologies of calcite phase for two methods. As observed from Fig. 8A, the presence of ultrasound leads to a formation of rhombic $CaCO_3$ particles with sharp edges which are randomly stacked and densely distributed. Whereas in the absence of ultrasound, scalenohedral $CaCO_3$ particle formation is predominant with larger particle size (Fig. 8B). As compared to previous results two totally

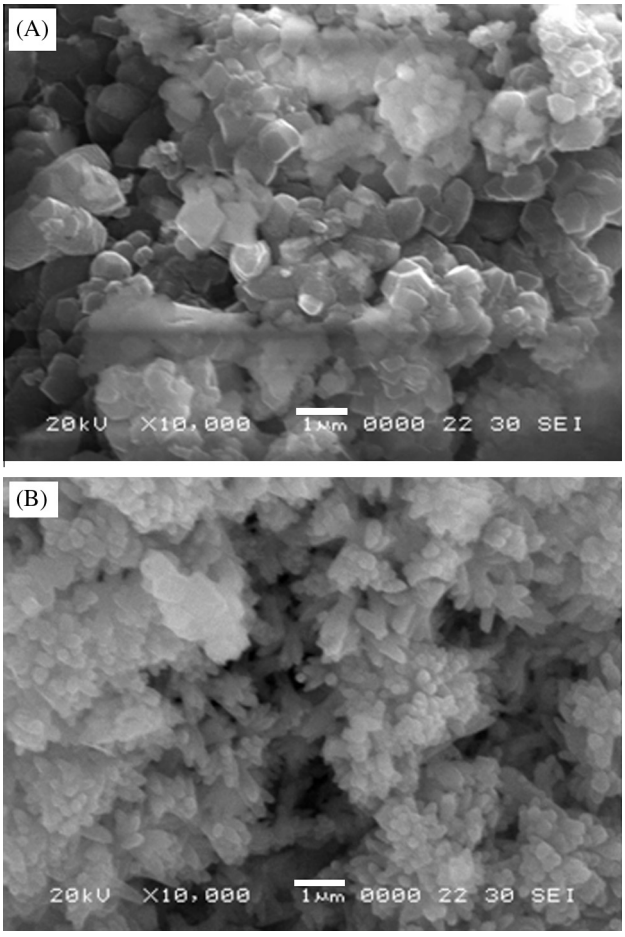

Fig. 8. SEM images of $CaCO_3$ particles for 16 mL/min $Ca(OH)_2$ slurry flow rate (A) ultrasound, and (B) stirring.

different morphologies are seen in this case. It is commonly believed that spindle shape is formed by the aggregation of primary particles in a preferential direction, and $CaCO_3$ primary particles have some sort of anisotropy [44]. This might be the possible reason for spindle like morphology of $CaCO_3$ particles in this case. At 16 mL/min $Ca(OH)_2$ slurry flow rate (3.85 wt% $Ca(OH)_2$ slurry concentration and CO_2 flow rate 45 LPH), the residence time of the reaction mixture in the reactor is higher which may promote the adsorption of primary particles in a preferential direction.

With both the synthesis methods, increase in the slurry flow rate results in reduced particle size. As the slurry flow rate is increased, the mean residence time of the reaction mixture in the reactor reduced which results into smaller particle size. As compared to conventional stirring, the smaller size of particles is achieved in the presence of ultrasound. This may be because of the effect of ultrasound which can result in faster reactions. When the CO_2 bubble size is smaller, the overall gas–liquid interfacial area is higher than the surface area of bigger bubbles [40]. Production of fine bubbles of CO_2 under the cavitating environment was found to be favorable for the dispersion and mass transfer of CO_2 which may have resulted in the intensification of the carbonation process and the formation of very fine $CaCO_3$ particles [8].

4. Conclusion

The continuous precipitation of calcium carbonate particles was successfully accomplished in CSTR in the presence and absence of ultrasonic environment. The analysis of conductivity-time curves

indicated the onset of nucleation and crystal growth. The effect of various operating parameters such as $Ca(OH)_2$ slurry concentration, CO_2 flow rate and $Ca(OH)_2$ slurry flow rate on the particle size and morphology of $CaCO_3$ was investigated with both the methods of preparation. The smaller particles of calcium carbonate were synthesized with the assistance of ultrasonication as against conventional method of preparation. The particle size is found to be reduced with an increase in the concentrations of $Ca(OH)_2$ and increasing CO_2 flow rate with both the methods. The slurry flow rate had a major effect on the particle size and the particle size reduced with increased slurry flow rate. Only calcite phase of $CaCO_3$ was predominantly present as confirmed by the characterization techniques. In most of the cases rhombohedral calcite particles formation were observed. As large quantities of $CaCO_3$ are required in industries and the production of calcium carbonate is mainly done in batch processes it would be an added advantage to get more quantity. Also in batch process an ultrasound probe system with limited power output and shorter sonication time can induce reaction crystallization in 1 liter of solution, therefore this continuous process may be feasible for industrial applications.

References

[1] P.C. Chen, C.Y. Tai, K.C. Lee, Morphology and growth rate of calcium carbonate crystals in a gas–liquid-solid reactive crystallizer, Chem. Eng. Sci. 52 (1997) 4171–4177.

[2] K. Sawada, The mechanisms of crystallization and transformation of calcium carbonates, Pure Appl. Chem. 69 (1997) 921–928.

[3] S. Zhang, X. Li, Synthesis and characterization of $CaCO_3$@SiO_2 core–shell nanoparticles, Powder Technol. 141 (2004) 75–79.

[4] M. Vucak, M.N. Pons, J. Peric, H. Vivier, Effect of precipitation conditions on the morphology of calcium carbonate: quantification of crystal shapes using image analysis, Powder Technol. 97 (1998) 1–5.

[5] M. Kitamura, H. Konno, A. Yasui, H. Masuoka, Controlling factors and mechanism of reactive crystallization of calcium carbonate polymorphs from calcium hydroxide suspensions, J. Cryst. Growth 236 (2002) 323–332.

[6] R.Y. Lin, J.Y. Zhang, Y.Q. Bai, Mass transfer of reactive crystallization in synthesizing calcite nanocrystal, Chem. Eng. Sci. 61 (2006) 7019–7028.

[7] O. Sohnel, J.W. Mullin, Precipitation of calcium carbonate, J. Cryst. Growth 60 (1982) 239–250.

[8] L. Xiang, Y. Xiang, Y. Wen, F. Wei, Formation of $CaCO_3$ nanoparticles in the presence of terpineol, Mater. Lett. 58 (2004) 959–965.

[9] J. Gomez-Morales, J. Torrent-Burgues, A. Lopez-Macipe, R. Rodriguez-Clemente, Precipitation of calcium carbonate from solutions with varying Ca^{2+}/carbonate ratios, J. Cryst. Growth 166 (1996) 1020–1026.

[10] V.A. Juvekar, M.M. Sharma, Absorption of CO_2 in a suspension of lime, Chem. Eng. Sci. 28 (1973) 825–837.

[11] M.V. Dagaonkar, A. Mehra, R. Jain, H.J. Heeres, Synthesis of $CaCO_3$ nanoparticles by carbonation of lime solutions in reverse micellar systems, Chem. Eng. Des. 82 (A11) (2004) 1438–1443.

[12] M. He, E. Forssberg, Ultrasonication-assisted synthesis of calcium carbonate nanoparticles, Chem. Eng. Commun. 192 (2005) 1468–1481.

[13] S.H. Sonawane, S.R. Shirsath, P.K. Khanna, S. Pawar, C.M. Mahajan, V. Paithankar, V. Shinde, C.V. Kapadnis, An innovative method for effective micro-mixing of CO_2 gas during synthesis of nano-calcite crystal using sonochemical carbonization, Chem. Eng. J. 143 (2008) 308–313.

[14] S. Wachi, A.G. Jones, Effect of gas–liquid mass transfer on crystal size distribution during the batch precipitation of calcium carbonate, Chem. Eng. Sci. 46 (1991) 3289–3293.

[15] W.M. Jung, S.H. Kang, W.S. Kim, C.K. Choi, Particle morphology of calcium carbonate precipitated by gas–liquid reaction in a Couette–Taylor reactor, Chem. Eng. Sci. 55 (2000) 733–747.

[16] J. Hostomskyt, A.G. Hostomskyt, Calcium carbonate crystallization, agglomeration and form during continuous precipitation from solution, J. Phys. D Appl. Phys. 24 (1991) 165–170.

[17] H. Yagi, A. Iwazawa, R. Sonobe, T. Matsubara, H. Hikila, Crystallization of calcium carbonate accompanying chemical absorption, Ind. Eng. Chem. Fundam. 23 (1984) 153–158.

[18] D. Chakraborty, V.K. Agarwal, S.K. Bhatia, J. Bellare, Steady-state transitions and polymorph transformations in continuous precipitation of calcium carbonate, Ind. Eng. Chem. Res. 33 (1994) 2187–2197.

[19] R. Rodriguez-Clemente, J. Gomez-Morales, Microwave precipitation of $CaCO_3$ from homogeneous solutions, J. Cryst. Growth 169 (1996) 339–346.

[20] R. Vacassy, J. Lemaitre, H. Hofmann, J.H. Gerlings, Calcium carbonate precipitation using new segmented flow tubular reactor, AIChE J. 46 (2000) 1241–1252.

[21] R.Y. Lin, J.Y. Zhang, P.X. Zhang, Nucleation and growth kinetics in synthesizing nanometer calcite, J. Cryst. Growth 245 (2002) 309–320.

[22] Z. Ji, Z. Liu, F. He, Synthesis of nanosized $BaSO_4$ and $CaCO_3$ particles with a membrane reactor: effects of additives on particles, J. Colloid Interface Sci. 266 (2003) 322–327.

[23] M.D.L. de Castro, F. Priego-Capote, Ultrasound-assisted crystallization (sonocrystallization), Ultrason. Sonochem. 14 (2007) 717–724.

[24] H. Oubani, A. Abbas, M. Srour, J.A. Romagnoli, Effects of operating conditions on particle size in sonocrystallization, Asia-Pac. J. Chem. Eng. 5 (2010) 599–608.

[25] A. Kumar, P. Gogate, A.B. Pandit, A.M. Wilhelm, H. Delmas, Investigation of induction of air due to ultrasound source in the sonochemical reactors, Ultrason. Sonochem. 12 (2005) 453–460.

[26] N. Lyczko, F. Espitalier, O. Louisnard, J. Schwartzentruber, Effect of ultrasound on the induction time and the metastable zone widths of potassium sulphate, Chem. Eng. J. 86 (2002) 233–241.

[27] D. Gomez-Diaz, J.M. Navaza, B. Sanjurjo, Analysis of mass transfer in the precipitation process of calcium carbonate using a gas/liquid reaction, Chem. Eng. J. 116 (2006) 203–209.

[28] S. Zhang, Y. Han, J. Jiang, H. Wang, Studies of crystallization of nano-calcium carbonate in the reaction system $Ca(OH)_2$–H_2O–CO_2, J. Northeastern Univ. Nat. Sci. 21 (2000) 169–172.

[29] M. Vucak, J. Peric, R. Krstulovic, Precipitation of calcium carbonate in a calcium nitrate and monoethanolamine solution, Powder Technol. 91 (1997) 69–74.

[30] P.D. Silva, L. Bucea, D.R. Moorehead, V. Sirivivatnanon, Carbonate binders: reaction kinetics, strength and microstructure, Cement Concr. Compos. 28 (2006) 613–620.

[31] D. Shan, M. Zhu, H. Xue, S. Cosnier, Development of amperometric biosensor for glucose based on a novel attractive enzyme immobilization matrix: calcium carbonate nanoparticles, Biosens. Bioelectron. 22 (2007) 1612–1617.

[32] Q. Sun, Y. Deng, Synthesis of micrometer to nanometer $CaCO_3$ particles via mass restriction method in an emulsion liquid membrane process, J. Colloid Interface Sci. 278 (2004) 376–382.

[33] M.A. Patel, B.A. Bhanvase, S.H. Sonawane, Production of cerium zinc molybdate nano pigment by innovative ultrasound assisted approach, Ultrason. Sonochem. 20 (2013) 906–913.

[34] F.B. Reig, J.V. Gimeno Adelantado, M.C.M. Moya Moreno, FTIR quantitative analysis of calcium carbonate (calcite) and silica (quartz) mixtures using the constant ratio method. Application to geological samples, Talanta 58 (2002) 811–821.

[35] N.V. Vagenas, A. Gatsouli, C.G. Kontoyannis, Quantitative analysis of synthetic calcium carbonate polymorphs using FT-IR spectroscopy, Talanta 59 (2003) 831–836.

[36] W. Gu, Douglas W. Bousfield, Carl P. Tripp, Formation of calcium carbonate particles by direct contact of $Ca(OH)_2$ powders with supercritical CO_2, J. Mater. Chem. 16 (2006) 3312–3317.

[37] Nishida, Precipitation of calcium carbonate by ultrasonic irradiation, Ultrason. Sonochem. 11 (2004) 423–428.

[38] N. Enomoto, J. Akagi, Z. Nakagawa, Sonochemical powder processing of iron hydroxides, Ultrason. Sonochem. 3 (1996) S97–S103.

[39] Y. Wen, L. Xiang, Y. Jin, Synthesis of plate-like calcium carbonate via carbonation route, Mater. Lett. 57 (2003) 2565–2571.

[40] B. Feng, A.K. Yong, H. An, Effect of various factors on the particle size of calcium carbonate formed in a precipitation process, Mater. Sci. Eng., A 445–446 (2007) 170–179.

[41] H. Li, H. Li, Z. Guo, Y. Liu, The application of power ultrasound to reaction crystallization, Ultrason. Sonochem. 13 (2006) 359–363.

[42] Y.S. Han, G. Hadiko, M. Fuji, M. Takahashi, Effect of flow rate and CO_2 content on the phase and morphology of $CaCO_3$ prepared by bubbling method, J. Cryst. Growth 276 (2005) 541–548.

[43] T. Thriveni, N. Um, S.Y. Nam, Y.J. Ahn, C. Han, J.W. Ahn, Factors affecting the crystal growth of scalenohedral calcite by a carbonation process, J. Korean Ceram. Soc. 51 (2014) 107–114.

[44] K. Kadota, T. Yamamoto, A. Shimosaka, Y. Shirakawa, J. Hidaka, M. Kouzu, Aggregation modeling of calcium carbonate particles by Monte Carlo simulation, J. Nanopart. Res. 13 (2011) 7209–7218.